

# Evaluation of the Mode *I* Plastic Zone Size at the Crack Tip Using RKPM and FEM

Masood Hajali<sup>1</sup>, Caesar Abishdid<sup>2</sup>

<sup>1</sup>PhD Candidate, Department of Civil and Environmental Engineering, Florida International University, Miami, Florida 33174, Phone: (954)849-0078, E-mail: [mhaja002@fiu.edu](mailto:mhaja002@fiu.edu)

<sup>2</sup>Director of External Programs, College of Engineering and Computing, Florida International University, Miami, Florida 33174, Fax: (305)348-2802, E-mail: [abishdid@fiu.edu](mailto:abishdid@fiu.edu)

## Abstract

In recent years, much research have been done on mesh-free methods for solving differential equation problems including crack and also obtained satisfactory results. Among these methods Reproducing Kernel Particle Method (RKPM) has been used increasingly in fracture mechanic problems. RKPM is a meshfree technology which has proven very useful for solving problems of fracture mechanics. In this study, it is proposed to obtain the mode *I* plastic zone size and shape at the crack-tip in a work-hardening material using RKPM. Ramberg-Osgood stress-strain relation is assumed. Results including plastic zone shape are compared with finite element method (FEM) to show the accuracy of RKPM. Results show that the plastic zone size in crack tip for the plane-strain condition is bigger that plane-stress condition. The reason can be stated that in plane-strain condition due to limitations in third dimension, stress is created in the third dimension (*z*-direction) and cause to increase the daviatoric stress according to  $J_2$ -Deformational theory and also cause to increase in plastic zone size. The main objective is to obtain the mode *I* plastic zone shape at the crack-tip in a work-hardening material using RKPM and FEM.

**Keywords:** Reproducing Kernel Particle Method (RKPM), Mode *I* Crack, Plastic Zone Size, Finite Element Method, Crack Tip, Ramberg-Osgood.

## Introduction

Recently, meshfree methods are increasingly utilized in solving various types of boundary value problems. Meshfree methods eliminate some or all of the traditional mesh-based view of the computational domain and rely on a particle view of the field problem. One of the oldest approaches in meshfree methods is the Smooth Particle Hydrodynamics (SPH) which was first introduced in 1977 by Lucy Gingold and Monaghan [2]. SPH was first applied in astrophysics to model fluid dynamics phenomena. In 1993, Petschek [3] and Libersky extended SPH to solid mechanics. Recent advances on meshfree methods such as, element-free Galerkin method (EFGM) by Belytschko et al. [7] at 1994, reproducing kernel particle method (RKPM) by Liu, et al. [1] at 1996, meshless local Petrov-Galerkin (MLPG) by Atluri et al. [13] at 1999. Meshfree methods go back to the seventies. The major difference to finite element methods is that the domain of interest is discretized only with nodes, often called particles.

There have been two widely used treatments, namely visibility and diffraction for dealing with the internal discontinuity in fracture mechanics. Mesh-free methods go back to the seventies. The

major difference to finite element methods is that the domain of interest is discretized only with nodes, often called particles. In recent years, much research have been done on mesh-free methods for solving differential equation problems including crack and also obtained satisfactory results. Among these methods Reproducing Kernel Particle Method (RKPM) has been used increasingly in fracture mechanic problems. Boundary value problems (BVPs) often have essential boundary conditions (EBCs) that involve derivatives, for example, in beams and plates, where slopes are commonly enforced at the boundaries. Such problems are solved numerically using mesh-free techniques like the RKPM and the EFGM.

It is recognized that plastic deformation will occur at the crack tip as a result of the high stresses that are generated by the sharp stress concentration. To estimate the extent of this plastic deformation, Irwin equated the yield strength to the y-direction stress along the x-axis and solved for the radius. The radius value determined was the distance along the x-axis where the stress perpendicular to the crack direction would equal the yield strength; thus, Irwin found that the extent of plastic deformation was

$$r_y = \frac{1}{2\pi} \left( \frac{K}{\sigma_{ys}} \right)^2 \quad (1)$$

Subsequent investigations have shown that the stresses within the crack tip region are lower than the elastic stresses and that the size of the plastic deformation zone in advance of the crack is between  $r_y$  and  $2r_y$ . Models of an elastic, perfectly plastic material have shown that the material outside the plastic zone is stressed as if the crack were centered in the plastic zone. Figure1 describes a schematic model of the plastic zone and the stresses ahead of the crack tip.

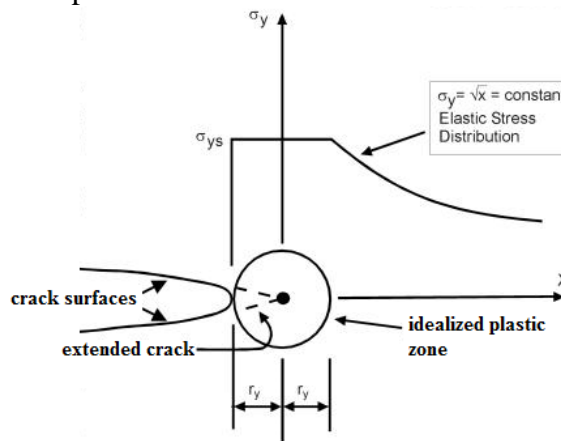


Figure1. Yield Model for Crack Tip

### Review of Reproducing Kernel Particle Method

SPH method first introduced in 1977 by Lucy Gingold and Monaghan [2]. In SPH method, system response is reproduced by invoking the notion of a kernel approximation for  $f(x)$  on domain  $\Omega$  by the following equation:

$$u^R(\xi) = \int_{\Omega} \phi_a(\xi - x) u(x) d\Omega \quad (2)$$

Where  $u^R(\xi)$  is the approximation function,  $\Omega$  is the domain of interest,  $\phi_a(\xi-x)$  is a kernel function, and  $a$  is the smoothing parameter. This method is not accurate on the boundary condition or when few particles are considered on the domain unless the lumped volume is carefully selected which is a very hard and time consuming work. RKPM is an alternative method to formulate the discrete consistency that is lacking in SPH method. The foundation of RKPM proposed by Liu et al. [1] in 1993 and was first applied to computational mechanics. RKPM modifies the kernel function by introducing a correction function  $C(\xi; \xi-x)$ . Adding the correction function in the kernel approximation significantly enhances the solution accuracy in comparison to SPH method. The method of using corrected kernel approximation in reproducing a function is called Reproducing Kernel Particle Method. The reproduced kernel function of  $u(x)$  can be written as:

$$u^R(\xi) = \int_{\Omega} u(x) \bar{\phi}(\xi; \xi-x) dx \quad (3)$$

Where  $\bar{\phi}_a(\xi; \xi-x)$  is the modified kernel function on domain  $\Omega$  that is expressed by:

$$\bar{\phi}(\xi; \xi-x) = C(\xi; \xi-x) \phi(\xi-x) \quad (4)$$

$$\phi_a(\xi-x_i) = \frac{1}{a} \phi\left(\frac{\xi-x_i}{a}\right) \quad (5)$$

Where  $\phi_a(\xi-x)$  is window function,  $C(\xi; \xi-x)$  is correction function, and  $a$  is the dilation parameter of the kernel function. Dilation parameter is defined in order to make more flexibility for the window function and this parameter will control the expansion of the window function on the domain. The correction function  $C(\xi; \xi-x)$  proposed by Liu et al. [1] is shown by a linear combination of polynomial including some unknown coefficients. These unknown coefficients will be computed after imposing the boundary conditions. Consider the following Taylor series expansion in order to get the equations for reproducing an arbitrary function:

$$u(x) = \sum_{\alpha=0}^{\infty} \frac{(-1)^{\alpha}}{\alpha!} (\xi-x)^{\alpha} u^{(\alpha)}(\xi) \quad (6)$$

Substituting Equation 6 into Equation 3 leads to:

$$u^R(\xi) = \sum_{\alpha=0}^{\infty} \frac{(-1)^{\alpha}}{\alpha!} \left( \int_{\Omega} (\xi-x)^{\alpha} \bar{\phi}_a(\xi; \xi-x) dx \right) u^{(\alpha)}(\xi) \quad (7)$$

In order to simplify the Equation 7, the  $\alpha$ th degree moment matrix of function  $\bar{\phi}_a(\xi; \xi-x)$  is defined by:

$$\bar{m}_{\alpha}(\xi) = \int_{\Omega} (\xi-x)^{\alpha} \bar{\phi}_a(\xi; \xi-x) dx \quad (8)$$

Then the Equation 7 will be rewritten in the following form:

$$u^R(\xi) = \bar{m}_o(\xi)u(\xi) + \sum_{\alpha=1}^{\infty} \frac{(-1)^\alpha}{\alpha!} \bar{m}_\alpha(\xi) u^{(\alpha)}(\xi) \quad (9)$$

In order to exactly reproduce nth order polynomials function, the following conditions need to be satisfied;

$$\begin{cases} \bar{m}_o(\xi) = 1 \\ \bar{m}_\alpha(\xi) = 0 \end{cases} \quad \alpha = 1, 2, \dots, n \quad (10)$$

Or in summary:

$$\bar{m}_\alpha(\xi) = \delta_{\alpha o} \quad ; \quad \alpha = 0, 1, 2, \dots, n \quad (11)$$

If a correction function including n+1 unknown coefficient is defined, n+1 equation of 11 can be satisfied simultaneously. The correction function is defined by:

$$C(\xi, \xi - x) = \sum_{\alpha=0}^n \beta_\alpha(\xi) (\xi - x)^\alpha \quad (12)$$

It can be also express in matrix form:

$$C(\xi, \xi - x) = \mathbf{P}^T(\xi - x) \boldsymbol{\beta}(\xi) \quad (13)$$

Where  $\mathbf{P}^T(\xi - x)$  is a set of basic functions and including n+1 components and  $\boldsymbol{\beta}(\xi)$  is a set of unknown coefficient. Substituting Equation 13 into Equation 11 and helping Equation 8 leads to:

$$\int_{\Omega} (\xi - x)^\alpha \bar{\phi}_a(\xi, \xi - x) dx = \delta_{\alpha o} \quad \alpha = 0, 1, 2, \dots, n$$

$$\int_{\Omega} \left\langle (\xi - x)^\alpha (\xi - x)^{\alpha+1} \dots (\xi - x)^{\alpha+n} \right\rangle \phi_a(\xi - x) dx \begin{Bmatrix} \beta_o(\xi) \\ \beta_1(\xi) \\ \vdots \\ \beta_n(\xi) \end{Bmatrix} \delta_{\alpha\alpha}$$

$$\alpha = 0, 1, 2, \dots, n \quad (14)$$

From the Equation 14 the unknown coefficient sets of  $\beta_i(\xi)$  is obtained. The Equation 14 can be also rewritten as Equation 16.

$$m_\alpha(\xi) = \int_{\Omega} (\xi - x)^\alpha \phi_a(\xi - x) dx \quad (15)$$

$$\mathbf{M}(\xi) \boldsymbol{\beta}(\xi) = \mathbf{P}(0) \quad (16)$$

Moment matrix M can be shown like:

$$\mathbf{M}(\xi) = \int_{\Omega} \mathbf{P}(\xi - x) \mathbf{P}^T(\xi - x) \phi_a(\xi - x) dx \quad (17)$$

Since the window function is always positive, all the components of moment matrix are linearly independent with respect to  $\phi_a$  therefore the moment matrix is nonsingular. Hence simultaneously solving Equation 16 the unknown coefficient sets of  $\beta_i(\xi)$  are obtained:

$$\boldsymbol{\beta}(\xi) = \mathbf{M}^{-1}(\xi) \mathbf{P}(0) \quad (18)$$

After obtaining the unknown coefficient sets  $\beta_i(\xi)$  the correction function can be easily calculated. Here sine and cosine functions are reproduced using 52 nodes in one period with dilation parameter of equal twice the distance between nodes (Figures 2 and 3).

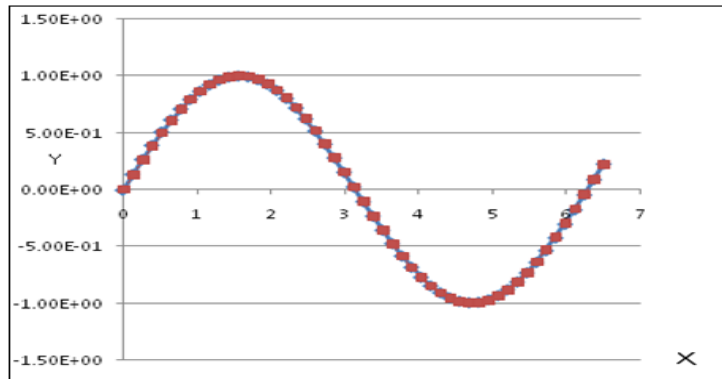


Figure2. Reproducing Sinuous function

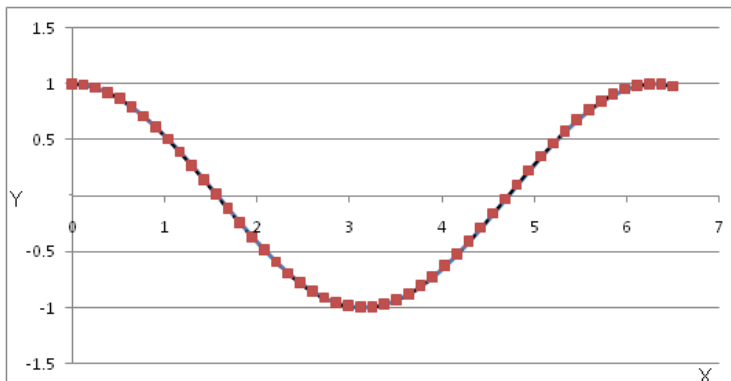


Figure3. Reproducing Cosines function

### Edge Crack Modeling in RKPM

With what was stated in previous, and using a FORTRAN program that was written for solving the liner elastic on a steel plate with specified dimension using RKPM. The stress, strain, and displacement field in x and y direction in all computational particles under plane-strain conditions were obtained. Penalty method is used to apply the boundary conditions. Penalty

coefficient,  $\beta$ , is adopted as  $10^6 E$ , in which  $E$  is Young's modulus. A rectangular steel plate is selected with dimensions of  $2.5 \times 5 \text{ cm}^2$  ( $2 \times 1 \text{ in}^2$ ). An edge crack is considered with a length of  $0.5 \text{ cm}$  ( $0.2 \text{ inch}$ ) in the middle of the plate. A tensile stress of  $70 \text{ MPa}$  ( $10 \text{ ksi}$ ) is applied at the bottom and the top of the plate. The loading increment is assumed  $7 \text{ MPa}$  ( $1 \text{ ksi}$ ). Roller constraint is used for the plane in front of the crack and pin constraint is used for the front face of the plate (Figure 4). Spline 3<sup>rd</sup> degree is used as a window function. The modulus of elasticity of the plate is  $207000 \text{ MPa}$  ( $30,000 \text{ ksi}$ ), Poisson ratio of  $0.3$  and hardening parameter  $n=10$ . The problem is investigated using  $800$  particles uniformly scattered on the surface of the plate, and  $53$  particles positioned on the circles with angles of  $45$  degree around the crack tip.

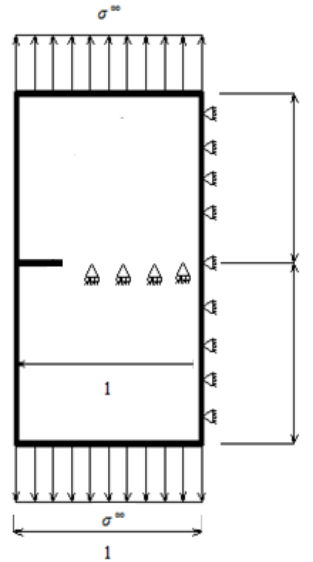


Figure4. Domain and Boundary Conditions

The FORTRAN program developed for the elastic-plastic material is able to recognize the yielded particles in according to Von-Mises criterion. For the same plate with dimensions  $2 \times 1$  including  $853$  particles, effective stress is shown for plane-strain conditions. The crack tip region was refined using more particles in the circle and star arrangements. In this problem, dilation parameter is  $0.1$  for the refined particles and is  $0.13$  for the rest of particles. Also, to have a better insight of stress distribution around the crack tip, the contours of the effective stresses are outlined in Figure 5.

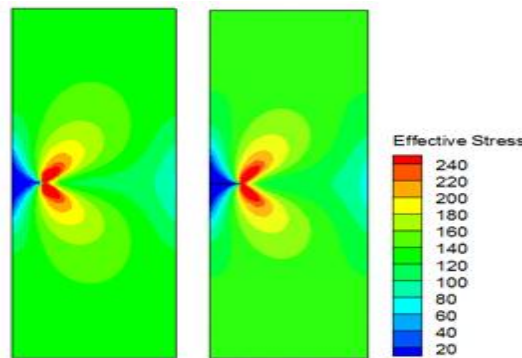


Figure5. Contours of Effective Stress using RKPM

## Finite Element Model

A numerical analysis was performed using finite element program ANSYS12 to exhibit the efficacy of RKPM in analyzing crack problems. The model considered the measured geometry, material properties and initial edge crack at the middle of the plate. Quadratic plane strain elements were used throughout the entire domain with a mesh size of  $0.01 \times 0.01$ . Ideal boundary conditions were chosen as shown in Figure 6. A cubic steel plate is selected with dimensions of  $2.5 \times 5 \text{ cm}^2$  ( $2 \times 1 \text{ in}^2$ ) and thickness of  $0.64 \text{ cm}$  ( $0.25 \text{ inch}$ ). An edge crack is considered with lengths of  $0.5 \text{ cm}$  and  $1 \text{ cm}$  ( $0.2$  and  $0.4 \text{ inch}$ ) in the middle of the plate. A tensile force of  $16191 \text{ N}$  ( $3640 \text{ lbs}$ ) is applied at the bottom and the top of the plate. 13045 elements are used for the sample with  $0.2W$  crack length. Finer mesh is used in the crack tip. Figures 7 and 8 show the stress and displacement contour in Y-direction throughout the plate. From Figure 7, it can be seen that the results of RKPM analysis are coincident with FEM results.

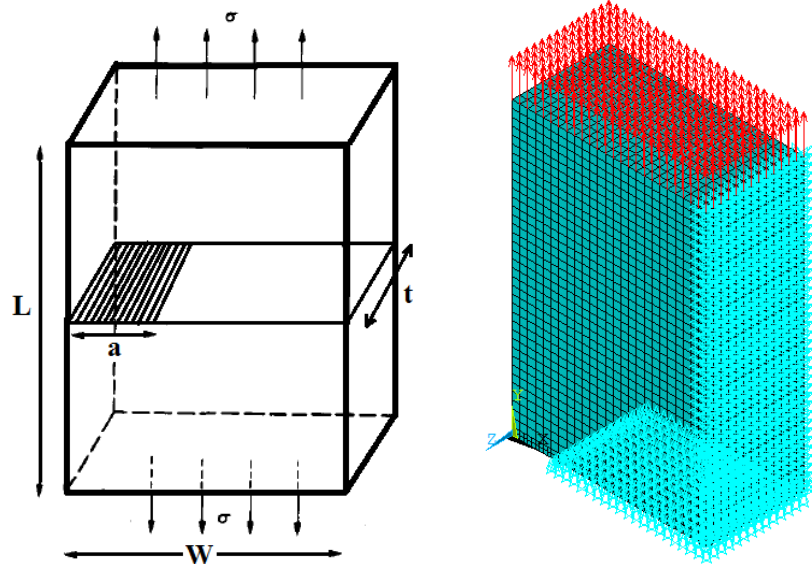
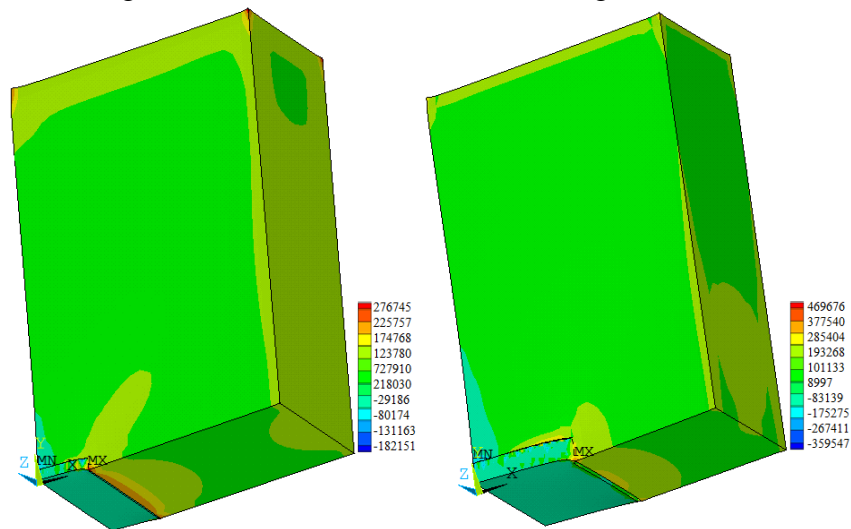


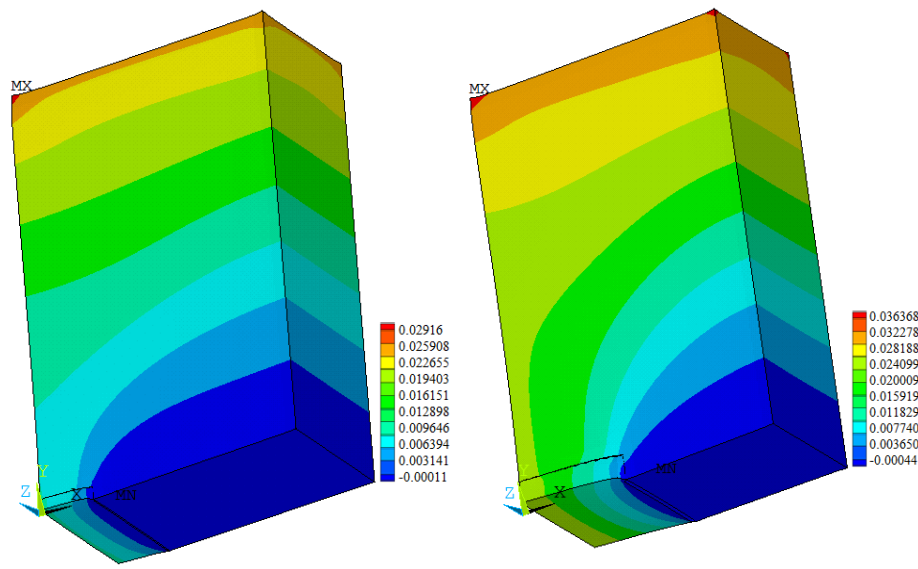
Figure6. 3-dimensional Crack Modeling in ANSYS



(a)  $a = 0.2W$

(b)  $a = 0.4W$

Figure7. Contours of Stress in Y-direction in psi



(a)  $a=0.2W$  (b)  $a=0.4W$   
 Figure8. Contours of Displacement in Y-direction in inch

### Conclusion

- 1) With increasing the degree of correction function in RKPM method, the number of Gaussian points needs to be increased to achieve more accurate answer. Also with increasing the number of Gaussian points, dilation parameter needs to be increased to achieve more accurate answer.
- 2) The plastic zone size in crack tip for the plane-stress condition is bigger than plane-strain condition. The reason can be stated that in plane-strain condition due to limitations in third dimension, stress is created in the third dimension (z-direction) and cause to decrease the deviatoric stress according to  $J_2$ -Deformational theory and also cause to decrease in plastic zone size.
- 3) Figures 2 and 3 show that only with 53 nodes we can exactly reproduce the sinuous and cosine functions using RKPM.

### References

1. Liu, W. K., Jun, S., Zhang, Y. F. (1995): "Reproducing Kernel Particles Methods." *International Journal for Numerical Methods in Fluids*, vol. 20, pp. 1081-1106.
2. Gingold, R.A. and Monaghan, J.J. (1977): "Smoothed particle hydrodynamics: theory and application to non-spherical stars." *Monthly Notices Royal Astronomical Society*, Vol. 181, pp. 375-389.
3. Libersky, L.D., Petschek, A.G. (1990): "Smooth particle hydrodynamics with strength of materials." *Advances in the Free Lagrange Method, Lecture Notes in Physics*, Vol. 395, pp. 248-257.
4. De Souza Neto, E. A., Peric, D., Owen, D. R. J. (2008), "Computational methods for plasticity: Theory and applications." *1st edition UK: WILEY*.



5. Jin, X.; Li, G.; Aluru, N. R. (2001): "On the equivalence between least-squares and kernel approximations in meshless methods." *Computer Modeling in Engineering and Sciences*, vol. 2, pp. 447-462.
6. Nguyen, V. P.; Rabczuk, T.; Bordas, S.; Duflot, M. (2008): "Meshless methods: A review and computer implementation aspects." *Mathematics and Computers in Simulation*, vol. 79, pp. 763-813.
7. Rao, B. N.; Rahman, S. (2004): "An enriched meshless method for non-linear fracture mechanics." *International Journal for Numerical Methods in Engineering*, vol. 59, pp. 197-223.
8. P. Niederegger, M. Knobloch, M. Fontana, (2006): "Elements with nonlinear stress-strain relationships subjected to local buckling." *Taylor & Francis Group, London*, ISBN 0-415-40817-2.
9. Rice, J. R. (1968), "A path independent integral and the approximate analysis of strain concentration by notches and cracks." *Journal of Applied Mechanics*, vol. 35, pp. 379-386.
10. Belytschko T., Y. Krongauz, D. Organ, M. Fleming, P. Krysl. Meshless Methods (1996): An overview and recent developments Computer methods in applied mechanics and engineering, Vol 139, pp3-47.
11. Simha, N. K.; Fischer, F. D.; Shan, G. X.; Chen, C. R.; Kolednik, O. (2008): *J* integral and crack driving force in elastic-plastic materials. *Journal of the Mechanics and Physics of Solids*, vol. 56, pp. 2876-2895.
12. Yuan, H.; Brocks, W. (1991): On the *J* integral concept for elastic-plastic crack extension. *Nuclear Engineering and Design*, vol. 131, pp. 157-173.
13. Zhu, T.; Atluri S. N. (1998): A modified collocation method and a penalty formulation for enforcing the essential boundary conditions in the element free Galerkin method. *Computational Mechanics*, vol. 21, pp. 211-222.
14. Zhu, T.; Zhang, J.; Atluri S. N. (1998): A local boundary integral equation (LBIE) method in computational mechanics, and a meshless discretization approach. *Computational mechanics*, vol. 21, pp. 223-235.